STATE OF ILLINOIS
WILLIAM G. STRATTON, *Governor*
DEPARTMENT OF REGISTRATION AND EDUCATION
VERA M. BINKS, *Director*

FLUID FLOW IN PETROLEUM RESERVOIRS

III. – Effect of Fluid-Fluid Interfacial Boundary Condition

Walter Rose

DIVISION OF THE
ILLINOIS STATE GEOLOGICAL SURVEY
JOHN C. FRYE, *Chief* URBANA

CIRCULAR 291 1960

CIRCULAR 291

ERRATA

Page 5. Top profile is figure 3. Bottom profile is figure 2. Captions remain in present position.

Page 6. Equation (8) should read

$$v_B = -\left[(dp/dx)_B/2\mu_B\right] \quad \left[y^2 - 2y\gamma + 2t\gamma - t^2\right] \qquad (8)$$

Page 8. Equation (11) should read

$$v_B = -\frac{(dp/dx)_B}{2\mu_B} \quad \left[\lambda^2 - 2\lambda\rho + 2\tau\rho - \tau^2\right] \qquad (11)$$

Page 14. Equation (20) should read

$$\frac{Li}{3t^3_M} + \frac{2Li}{3t^3_N} = \frac{(\Delta P)_{Li} W}{12Q_B\mu_B} \qquad (20)$$

Please enter these corrections in your copy.

FLUID FLOW IN PETROLEUM RESERVOIRS

III. — Effect of Fluid-Fluid Interfacial Boundary Condition

Walter Rose

ABSTRACT

Relative permeabilities greater than unity are predicted (for a reason different from that developed in Part I of this series), and it is shown that Darcy's Law does not accurately describe mixture flow phenomena in view of the nonzero velocity boundary condition that sometimes exists at the fluid-fluid interfacial boundaries. These indications are not to be gathered from examining available experimental data on relative permeability, but explanations are given to reconcile the discrepancy.

The analyses are based on mathematical models of reservoir rock porous media system. To the extent that the models and the reservoir prototype correspond, we can expect valid inferences that are important to an understanding of the mechanics of oil recovery processes. It is suggested that a flowing fluid has an increased mobility when surrounded (in part or entirely) by another immiscible fluid, whether the phenomenon is one of mixture flow in porous media or the transport of oil in a pipeline containing some annularly located water. The reported lubrication, moreover, is enhanced if the viscosity ratio of surrounding fluid to the flowing fluid has a low value.

INTRODUCTION

Previous papers in this series dealt with the fact that Kozeny-Carman theory leads to some unexpected predictions about the microscopics of mixture flow phenomena (Rose, 1957a, b). It was suggested that the relative oil permeability of reservoir rock, containing small amounts of connate water in pendular saturation configuration, might be greater than unity, in a way not anticipated from considerations of Darcy's Law. It also was suggested that some slightly consolidated sandstones might have a specific permeability greater than that of the unconsolidated sand from which they were derived.

A recent paper by Russell and Charles (1959) considers how a water layer on the internal surface of a pipe might serve as a "lubricant," thus lessening the power required to move oil through a pipe. The analyses given are limited to incompressible Newtonian fluids in laminar motion, and it is the phenomenon of transfer of viscous forces across fluid-fluid interfaces which gives rise to the reported effect.

In earlier work, Yuster (1951) discussed how the flow of fluid mixtures through porous media also might depend on the fact that a finite velocity must be taken as the boundary condition to be assigned at the fluid-fluid interfaces. By considering Poiseuille-type concentric flow in a circular tube to be a model of a porous medium saturated with two immiscible fluids, he concluded that the viscosity ratio of the two fluids would influence the volumetric throughput in a way indicating that Darcy's Law of flow could not be applied. His conclusion was contrary to experimental evidence, as Muskat's summary (1949) indicates; hence, it has become urgent to re-examine the theory descriptive of the flow of immiscible fluids through porous media.

A single liquid flowing without turbulence in a capillary tube (Poiseuille's Law) or in the interconnected and geometrically complicated interstices of porous media (Darcy's Law) has zero velocity at the solid phase boundaries (pore walls), with an ever-increasing velocity out towards the center of the pore space, because of viscous drag.

In mixture flow, however, the general condition is that each of the immiscible fluids is bounded by fluid-fluid interfaces, at least in part, and elsewhere is bounded by the pore walls. Yuster (1951) noted that there will usually be a nonzero velocity at the fluid-fluid interfaces; hence, Darcy's Law does not rigorously define the conductivity afforded by porous media to the flow of a given fluid which only partially saturates the pore spaces. Milne-Thomson (1955, p. 541) describes the boundary condition at an interface separating two fluids as one where the normal pressure and the viscous stress are continuous, provided surface tension is ignored. Similar recognition had been given by Hall (1956) who attempted to derive a Darcy Law formula applicable to multiphase saturated porous media.

As an attempt to reconcile Yuster's theoretical prediction (that mixture flow in porous media should be dependent upon viscosity ratio) with published laboratory data (which fail to show dependence on viscosity ratio), Scott and Rose (1953) chose to assume that Yuster's capillary tube model over-emphasized the magnitude of the ratio of fluid-fluid interfacial areas to fluid-solid surface areas. By replacing some of the fluid-fluid interface with a thin-walled tube, they were able to demonstrate that there would be a corresponding decrease in the dependence of fluid mixture conductivities upon the viscosity ratio.

The matter is by no means settled. Therefore, one purpose of this paper is to extend the analytical work of Russell and Charles (1959) and to apply the influence of fluid-fluid boundaries on mixture flow phenomena in other models of porous media prototypes. Another purpose of this paper is to provide analytical results useful for the solution of problems such as those already posed by Russell and Charles, and by Russell, Hodgson, and Govier (1959). Specifically, the "crack" model depicted in figure 1 is discussed for various boundary conditions of stratified flow between wide parallel plates.

In these connections, it should be noted that Yuster's concentric flow tube model is not one that can be evaluated easily by laboratory experiment. This is because both gravity and surface energy tend to cause the central filament of nonwetting fluid to be broken by the coalescence of the concentrically encompassing wetting fluid. Experimental verifications with the crack model are not handicapped by these factors, however (Ellis and Gay, 1959).

In another respect, the crack model is unique in having the flow of both fluids depend upon the viscosity ratio, as Russell and Charles (1959) show. By contrast, only the central fluid in the Yuster model flows in a way directly

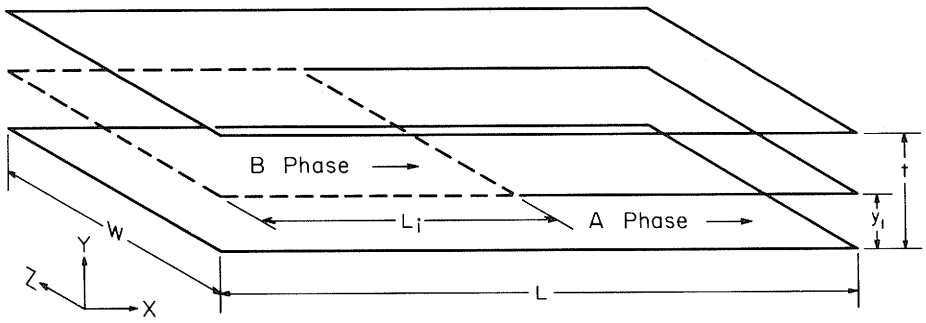

Fig. 1. The crack model having a total thickness of t and a boundary at Y_1 separating fluid phases A and B. L_i denotes the extent of the fluid-fluid boundary, and L is the over-all crack length. Flow is in the X-direction.

dependent upon viscosity ratio. Thus, the concentrically located surrounding fluid flows in a manner proportional to the factor $(r_o^2 - r^2)^2$, where r_o is the internal radius of the tube and r is the radial distance marking the location of the fluid-fluid interface. For comparable systems, this factor is always greater than that given by Lamb (1932) as:

$$(r_o^4 - r_i^4) - \left[(r_o^2 - r_i^2)^2 \;/\; \ln\ (r_o/r_i)\right]$$

for annular flow in an annulus of external radius, r_o, and internal radius, r_i; showing that lubrication of the outside liquid occurs in the Yuster model, albeit in a way not dependent upon the viscosity ratio of the inner to the outer fluid.

STRATIFIED LIQUID FLOW BETWEEN WIDE HORIZONTAL PARALLEL PLATES

Following the analytical methods of Russell and Charles (1959), equivalent but simplified expressions for the flow of the lower (liquid A) and upper (liquid B) fluids can be given as:

$$v_A = -(dp/dx) \;/\; (2\mu_A)\left[y^2 - y\beta\right] \tag{1}$$

$$v_B = -(dp/dx) \;/\; (2\mu_B)\left[y^2 - y\beta + t\beta - t^2\right] \tag{2}$$

$$Q_A = -(W\ dp/dx) \;/\; (12\mu_A)\left[3\beta Y_1^2 - 2Y_1^3\right] \tag{3}$$

$$Q_B = -(W\ dp/dx)/(12\mu_B)\left[4t^3 - 6t^2Y_1 + 2Y_1^3 - 3\beta(t - Y_1)^2\right] \tag{4}$$

where:

v = velocities;
Q = volumetric flow rate;
dp/dx = the pressure gradient acting in the direction of flow;
μ = viscosity;
y = the distance parameter in the vertical direction, having a value of zero at the bottom surface of the crack;

Y_1 = the value of "y" which marks the location of the fluid-fluid interface;
t = the value of "y" measuring the thickness of the crack;
W = the measure of the crack width in the horizontal direction normal to the direction of flow.

In these equations, the model of figure 1 is being considered, where viscous flow in the horizontal direction occurs because of terminal boundary conditions of pressure that develop the same pressure gradient in the upper and lower fluids. Also, in equations (1) through (4), the parameter, β, is defined by:

$$\beta = \left[(1 - \overline{\mu})\ Y_1^2 - t^2 \right] / \left[(1 - \overline{\mu})\ Y_1 - t \right] \qquad (5)$$

where $\overline{\mu}$ is the ratio of the viscosity of the upper to the lower fluid, μ_B/μ_A. Noting the limits of β as the viscosity ratio, $\overline{\mu}$, varies from zero through unity to infinity as:

$$\underset{\overline{\mu}\to 0}{\text{Limit}}\ \beta = (Y_1 + t) \cong t \ ; \quad \underset{\overline{\mu}\to 1}{\text{Limit}}\ \beta = t \ ; \quad \underset{\overline{\mu}\to \infty}{\text{Limit}}\ \beta = Y_1 \cong t$$

it follows that the parameter, β, serves to measure the effective thickness of the gap.

One advantage of equations (3) and (4) over the expressions given by Russell and Charles is that their algebraic form leads to the following cubic expression, from which the position of the interface for minimum power requirement can be derived as:

$$3\phi\ (d\beta/d\phi) + 6\beta - 6\phi = 0$$

where:

$$(d\beta/d\phi) = \frac{[(1 - \overline{\mu})\ \phi^2 - t^2]\ \ (1 - \overline{\mu}) - [(1 - \overline{\mu})\phi - t]\ \ (1 - \overline{\mu})\ \ (2\phi)}{[(1 - \overline{\mu})\ \ \phi - t]^2}$$

$$\phi = \left[\underset{\frac{dp}{dx}\ (Q_A + Q_B) \to \text{minimum}}{\text{Limit}} \right] Y_1 \qquad (6)$$

Figure 2 shows the velocity profiles predicted by equations (1) and (2) as obtained for values of $\overline{\mu}$ equal to 0.1, 1, and 10, respectively, when (Y_1/t) is 0.5.

For comparison, figure 3 shows the corresponding velocity profiles for the special case where no pressure energy is imparted to the lower (A) fluid directly so that $(dp/dx)_A$ is zero and $(dp/dx)_B$ is finite. In order to avoid a tilt of the fluid-fluid interface due to the unequal pressure gradients in fluids A and B, the fluids should have equal density; otherwise, the crack will have to be inclined, and gravity forces proportional to the density difference will have to be considered in the analysis.

Thus, by saying:

$$\mu_B \frac{d}{dy} \left[\frac{d\ v_B}{dy} \right] = (dp/dx)_B$$

$$\mu_A \frac{d}{dy} \left[\frac{d\ v_A}{dy} \right] = 0$$

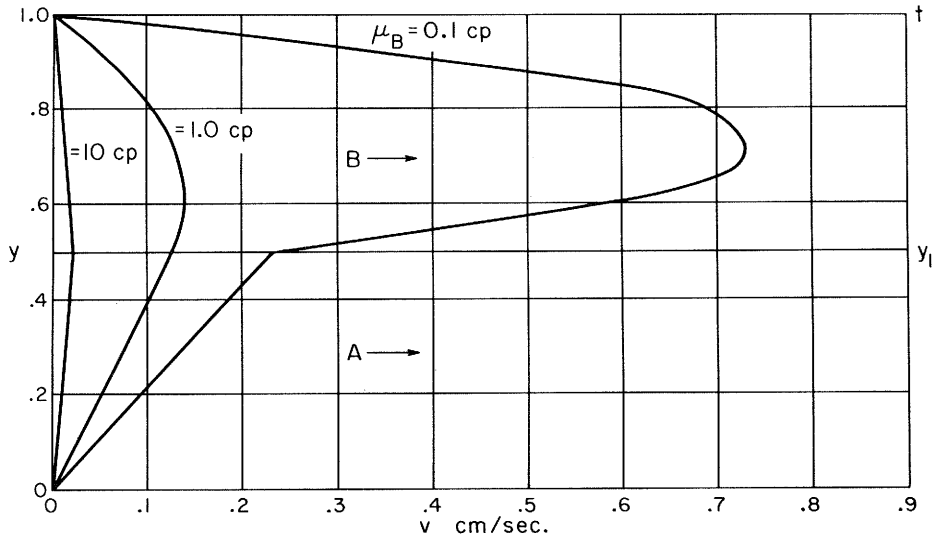

Fig. 2. Velocity profiles when $(dp/dx)_A = (dp/dx)_B$ = finite.

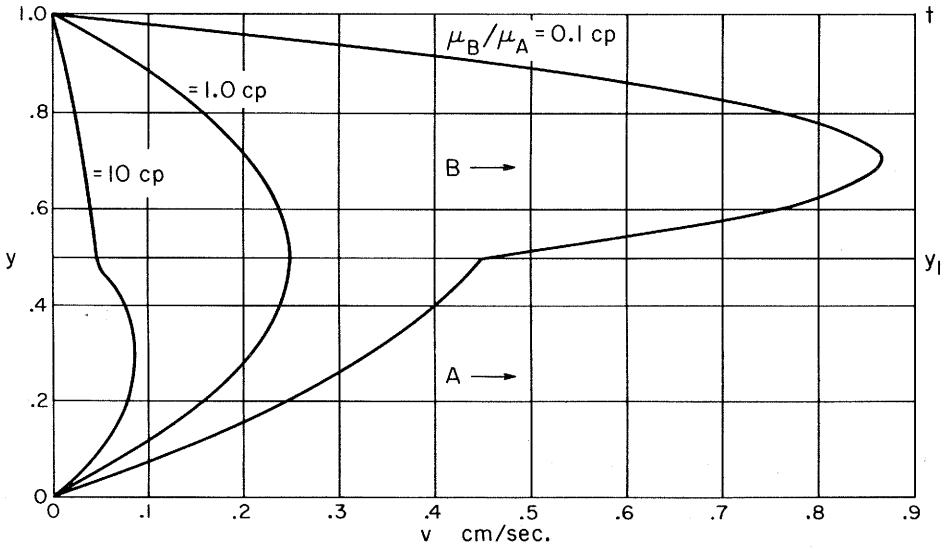

Fig. 3. Velocity profiles when $(dp/dx)_A = 0$ and there is no return of the A phase.

and imposing the boundary conditions which led to equations (1) and (2), the curves of figure 3 are given by:

$$v_A = -[(dp/dx)_B / \mu_A] \; [y \; (Y_1 - \gamma)] \tag{7}$$

$$v_B = -[(dp/dx)_B / \mu_B] \; [y^2 - 2y\gamma + 2t\gamma - t^2] \tag{8}$$

where:

$$\gamma = \frac{[(1 - 2\pi) \; Y_1^{\,2} - t^2]}{2 \, [(1 - \pi) \; Y_1 - t]}$$

Equation (7), of course, is a simple straight-line function, since movement of the lower fluid is by viscous drag, originating with the finite velocity of the upper liquid at the fluid-fluid interface and terminating with a zero velocity at the bottom boundary. Equation (8) closely corresponds, term by term, to equation (2), yielding a parabolic velocity distribution; hence, the parameter, γ, must have a significance corresponding to that assigned above to the parameter, β.

This modification, where the driving force is applied only to the upper fluid, means that there is an energy loss through the motion imparted by viscous drag to the lower fluid. This is shown, for example, by comparing figures 2 and 3 and noting that, for a given viscosity ratio condition, the velocities indicated in figure 3 are always less than those of figure 2. Also, deriving the volumetric throughputs corresponding to the conditions of equations (7) and (8) as:

$$Q_A = -\frac{W \; (dp/dx)_B}{4 \mu_A} \quad [Y_1^{\,2} \; (Y_1 - \gamma)] \tag{9}$$

$$Q_B = -\frac{W \; (dp/dx)_B}{6 \; \mu_B} \; [(2t^3 + Y_1^{\,3}) - 3\gamma(t - Y_1)^2 - 3t^2 Y_1] \tag{10}$$

it is again seen that Q_B by equation (10) is always less Q_B by equation (4), for all values of $(dp/dx)_B$.

In any case, it is worth while to realize that capillary systems can be found in nature and are to be encountered in industrial processes that contain two immiscible fluids, one moving in response to the action of some imposed force field and the other moving only because of viscous drag. For example, a hot vapor being pushed through the center of a tube will impart a forward motion to the liquid condensate that has formed on the cool tube walls. Similarly, in recovering oil from sedimentary rock, it sometimes happens that gravity acts to move one immiscible fluid through a porous region saturated with another immiscible fluid, which itself would be otherwise stationary because it is not directly acted upon by any other driving force.

Another case worth considering is one in which the upper fluid is given pressure energy to cause its movement, and movement in the lower fluid is due to the drag exerted across the fluid-fluid interface. In other words, $(dp/dx)_B$ is again finite and $(dp/dx)_A$ is zero but instead of having the lower fluid always moving forward with the upper fluid, provision is made for circulation of the lower fluid in a manner that can be taken as a model of an eddy swirl. Figure 4 shows the geometry of the system now being considered.

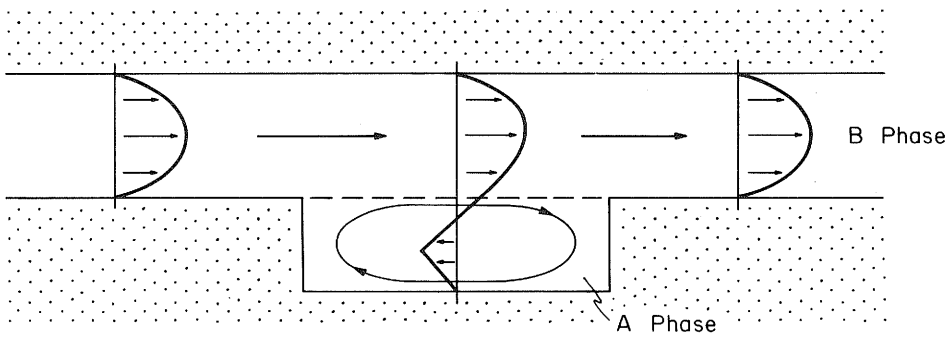

Fig. 4. The crack model with an eddy pocket containing the A phase circulating in a vortex-like motion. The B phase motion is described by a parabolic velocity profile except where separated from the A phase by a fluid-fluid interface, in which case the velocity profile of figure 5 applies.

One example of a system that can be recognized as the prototype of the model of figure 4 is the oil recovery system in which oil is flowing in the central pore spaces and here and there is moving over discontinuous elements of a wetting aqueous fluid held by capillary forces as pendular rings at points of particle contact (or as the filling of cul-de-sac pores). The wetting liquid in each disconnected pore space necessarily rotates when the continuous nonwetting fluid flows past the fluid-fluid boundary.

In the approximation of what happens when a flowing fluid imparts an eddy swirl to the adjacent immiscible fluid, it is assumed that the swirl is comprised of four principle directions of motion, as depicted in figure 4. Thus, in the upper center portion, phase A will be flowing in the same direction as phase B, and in the lower central portion of the eddy pocket, the motion is in the opposite direction. This latter provides for a return of the swirling fluid. Elsewhere phase A will be moving either downward (at the downstream end of the pocket) or upward (at the upstream end), such that in these regions there will be no horizontal component of velocity. In any case, a material balance holds everywhere.

Considering the transfer of fluid A, it is evident that the volume of fluid moving in the upper central portion in the direction of fluid B, must be equal to the volume being returned via the lower portion; that is, there will be a level in phase A (between $y = 0$ and $y = Y_1$) where the velocity of phase A is zero. As no discontinuity in the velocity profile should be assumed at this level, the velocity of fluid A will be seen to pass smoothly from negative (through zero) to positive values as y increases. It may further be assumed that the velocity profile of the negative velocities in the lower portion (where phase A is swirling back towards the high pressure end of the crack) will be represented by the isosceles triangle shown in figure 5. Thus, from geometry, the boundary condition is imposed that $v_A = 0$ at $y = 0.586\ Y_1$, as well as the other boundary conditions that:

$$v_A = 0 \text{ at } y = 0$$
$$v_B = v_A \text{ at } y = Y_1$$
$$v_B = 0 \text{ at } y = t$$

This case is discussed by Ellis and Gay (1959).

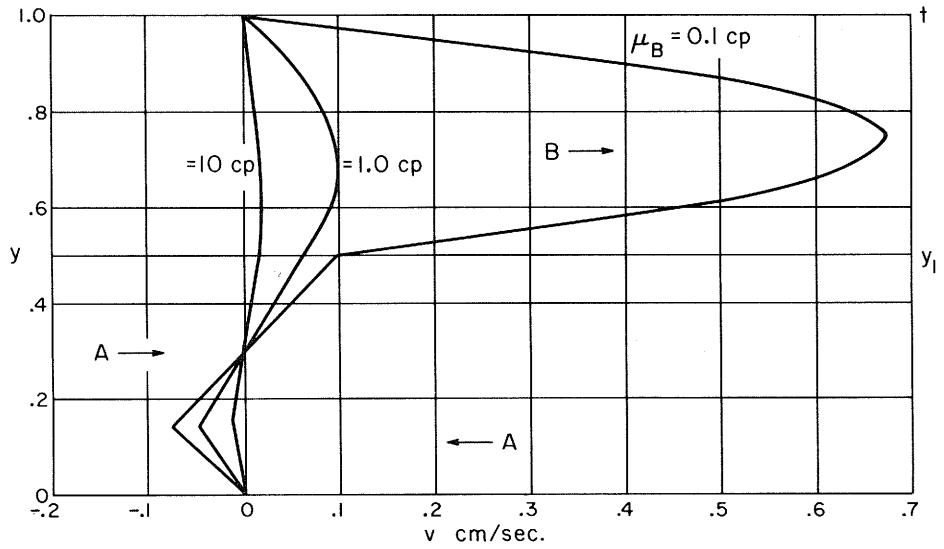

Fig. 5. Velocity profiles when $(dp/dx)_A = 0$ and there is a return of the A phase.

Now, introducing the notation:

$$\tau = t - 0.586\, Y_1$$

$$\lambda_1 = 0.414\, Y_1$$

$$\lambda = y - 0.586\, Y_1$$

$$\rho = \frac{[(1 - 2\bar{\mu})\ \lambda_1^2 - \tau^2]}{2\,[(1 - \bar{\mu})\ \lambda_1 - \tau]}$$

the velocity in fluid B, by analogy to equation (8), is given by:

$$v_B = -\frac{(dp/dx)_B}{2\,\mu_B}\qquad [\lambda^2 - 2\lambda + 2\,\tau\rho - \tau^2] \tag{11}$$

which is the function plotted for several viscosity ratios in figure 5. The positive and negative segments of the velocity profile for fluid A, of course, have a form as predicted from equations analogous to equation (7). Also for this case:

$$Q_B = -\frac{W\ (dp/dx)_B}{6\,\mu_B}\qquad [(2\tau^3 + \lambda_1^3) - 3\rho(\tau - \lambda_1)^2 - (3\tau^2\lambda_1)] \tag{12}$$

Comparison of equations (12), (10), and (4) show that for given conditions of $\bar{\mu}$, μ_B, and (Y_1/t), a given energy input (as measured by dp/dx) gives less throughput of fluid B when an eddy swirl developes (fig. 5) than when fluid A is simply dragged along (fig. 3), and the latter, in turn, gives less throughput than when dp/dx is acting directly on both fluids (fig. 2).

DISCUSSION

In order to examine the magnitude of the lubrication effect which gives fluid saturants of porous media (and other capillary systems such as tubes and cracks) an apparent increased mobility because of the fluid-fluid interfacial boundaries, the following notation is introduced:

$S_A = Y_1/t$ = the fractional saturation of the A fluid.

$S_B = (t - Y_1)/t$ = the fractional saturation of the B fluid.

L_i/L = length of the fluid-fluid interface/total path length.

$A_i = LiW$ = the area of the fluid-fluid interfacial boundary.

$A_s = (2L - Li)W$ = the area of the solid (pore walls) boundaries for values of S less than unity.

$A_T = 2LW$ = the total solid area when $S = 1$.

$A_i/A_T = Li/2L$

$A_s/A_T = (2L - Li)/(2L)$

$K_{RA} = \left[\dfrac{Q_A}{\underset{S_A = 1}{\text{Lim } Q}}\right]$ = fractional conductivity of fluid A.

$K_{RB} = \left[\dfrac{Q_B}{\underset{S_B = 1}{\text{Lim } Q}}\right]$ = fractional conductivity of fluid B.

The S terms are the familiar saturation terms, used in porous media theory, which measure the fraction of the pore space filled by the pore saturant. The K_R terms are the relative permeability parameters which measure the ratio of conductivity afforded by porous media to the flow-transfer of a pore saturant at some value of S (equal to or less than unity) to the conductivity afforded to the flow-transfer of the same saturant when its saturation is unity.

Heretofore (Muskat, 1949), theoretical deduction and experimental data commonly have been taken to indicate that relative permeabilities are explicit functions of saturation alone and are implicit functions of saturation distribution (as follows from the possibility of saturation hysteresis); but Yuster (1951) has indicated that the viscosity ratio, $\overline{\mu}$, may also be a determining factor. This possibility is now examined.

Equations (3) and (4) yield:

$$K_{RA} = \frac{3S_A^{\,2}\left[S_A^{\,2}(1 - \overline{\mu}) - 1\right] - 2S_A^{\,3}\left[S_A(1 - \overline{\mu}) - 1\right]}{S_A(1 - \overline{\mu}) - 1} \tag{13}$$

$$K_{RB} = S_B^{\,2}\left[\frac{S_B^{\,2}(1 - \overline{\mu}) + 2S_B - 3}{S_B(1 - \overline{\mu}) - 1}\right] \tag{14}$$

for the case where $(dp/dx)_A = (dp/dx)_B > 0$. Figure 6 shows that the conductivity of both the A and B fluids indeed are increased as the viscosity of the contiguous phase decreases (the upper curves) over the values which would be expected if Darcy's Law was applicable in describing mixture flow phenomena (the lowest curve of figure 6).

In fact, it is shown in figure 6 that whenever the viscosity ratio differs from unity, there will be a range of saturation values where the more viscous fluid flows more readily (K_R is greater than unity) than if this fluid completely filled the pore spaces (its saturation were unity). For the model described by equations (13) and (14), a maximum of a four-fold increase in conductivity of the more viscous phase is approached as the viscosity ratio approaches zero.

Comparison of the relative permeability curves of figure 6 with the experimental data cited by Muskat (1949) suggests the need for introducing a correction factor if better correspondence between model and prototype is to be achieved. The approach of Scott and Rose (1953) can be followed for this purpose, for it is clear that the models of figures 1 and 4 (as well as the capillary tube model discussed by Yuster [1951] and Russell and Charles [1959]) are defective in suggesting that the term, A_i/A_T, is unity for all values of saturation.

Thus, equation (14) may be revised as:

$$K_{RB} = \frac{S_B^{\,3}\,[S_B^{\,2}\,(1-a) + 2S_B - 3]}{\left(\frac{Li}{L}\right) S_B\,[S_B(1-a) - 1] + \left(\frac{L - Li}{L}\right)[S_B^{\,2}\,(1-a) + 2S_B - 3]} \qquad (15)$$

where $a = (\mu)^{-1} = (\mu_A/\mu_B)$

and figure 7 shows a significantly diminished dependence of the relative permeability function on viscosity ratio, as compared to figure 6, upon making some reasonable assumptions about the surface area functions, as:

$$(Ai/A_T)_W = 0.715\,(1 - S_W)$$
$$\text{and} \quad (A_s/A_T)_W = 0.715\,S_W + 0.285 \qquad (16)$$

where the subscript W identifies the B fluid as the wetting phase (cf. discussion in connection with equation [22] below).

In fact, no values of K_R greater than unity exist for this case, even when the viscosity ratio is most unfavorable (approaching zero), a result to be anticipated from an examination of extant experimental data.

Corresponding to equation (14), equation (10) yields:

$$K_{RB} = S_B^{\,3}\left[\frac{S_B\,(4-a) - 4}{S_B\,(1-a) - 1}\right] \qquad (17)$$

for the model where $(dp/dx)_A$ is zero, and fluid A is dragged forward by the motion of fluid B being acted upon by a finite $(dp/dx)_B$. Figure 8, a plot of equation (17), upon comparison with the corresponding curves of figure 6, shows a similar, albeit diminished dependence on viscosity ratio.

Of more immediate interest, however, are the functions to be derived from equation (12), for these describe the characteristics of the model in which a continuous flowing fluid (for example fluid B) imparts an eddy swirl to contiguous but

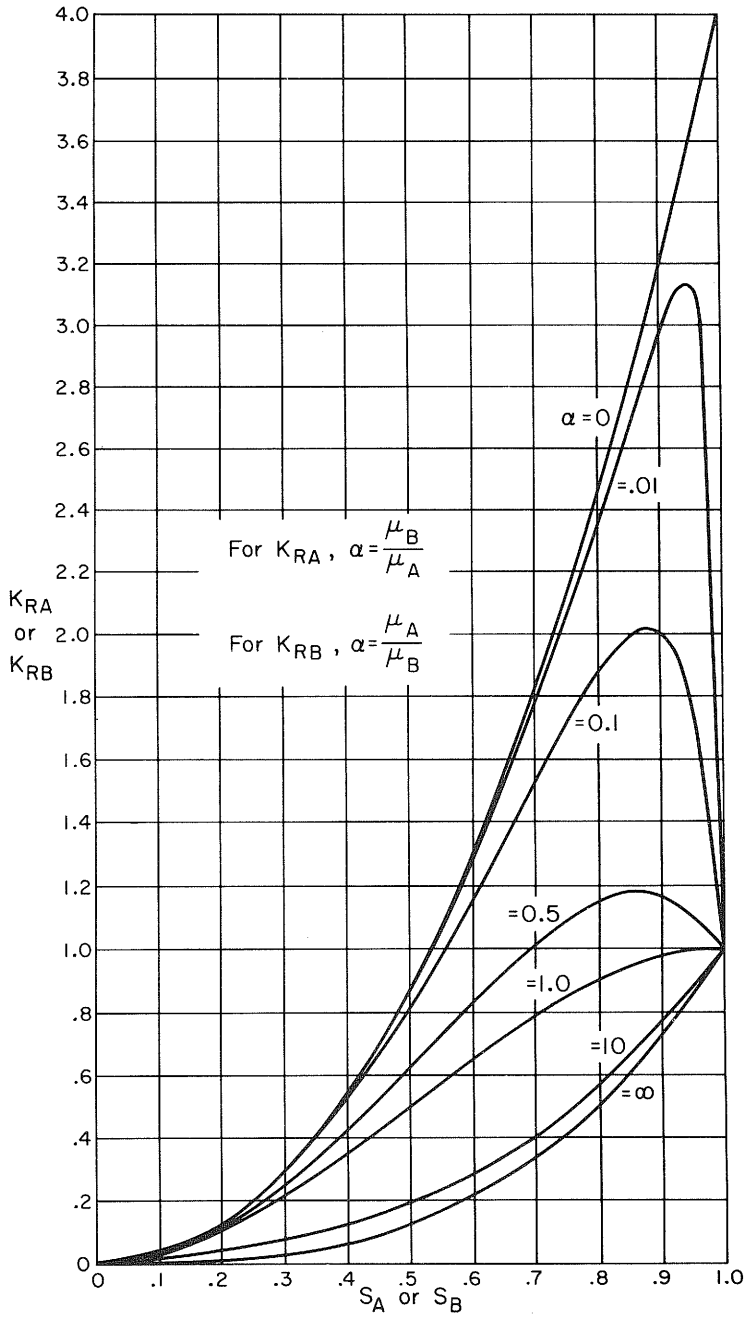

Fig. 6. Relative permeability curves for phases A and B using the model of figure 1 with $L_i = L$ at all saturations and $(dp/dx)_A = (dp/dx)_B$.

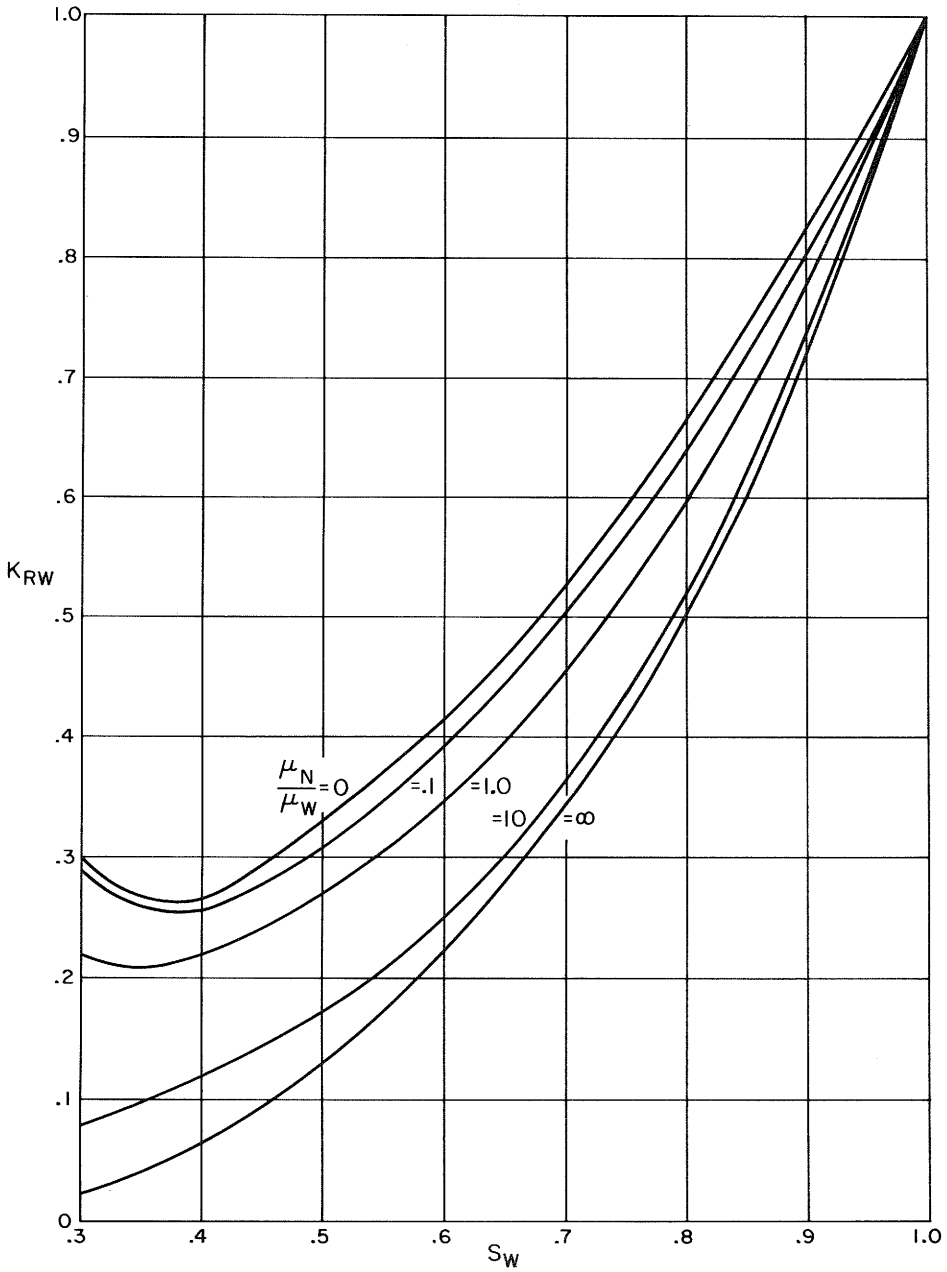

Fig. 7. Relative permeability curves for the wetting phase for the model of figure 1 in a special case, showing a greater dependence on viscosity ratio and proving the necessity for assuming the existence of eddy pockets.

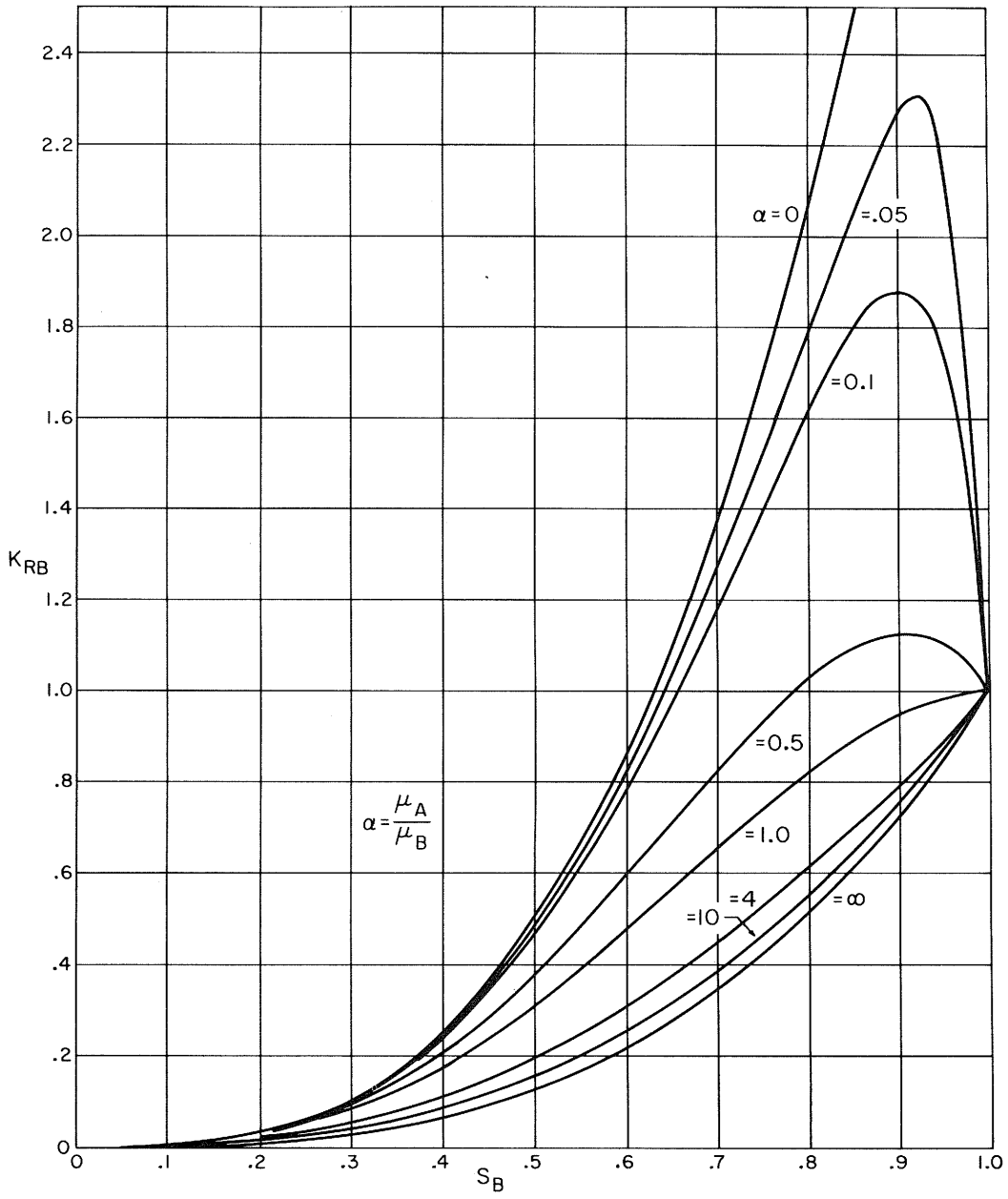

Fig. 8. Relative permeability curves for phase B using the model of figure 1 where $L_i = L$ for all saturations for the special case where $(dp/dx)_A = 0$ and there is no return of the A phase.

disconnected elements of an immobile pore saturant. As noted above, prototypes of this model occur widely and are of special importance in oil recovery systems.

Equation (12) gave the flow rate of the continuous phase as it exists over the central portion of the eddy pocket (fig. 4). Assuming that two-thirds of the fluid-fluid interface represents regions where there is no horizontal component of velocity in the A phase, and that in the remaining one-third central region where the A phase is being dragged in the direction of the motion of B (in the upper portion) or returning in the opposite direction (in the lower portion of the eddy pocket), it follows that for $L_i = L$ for all saturations, then:

$$K_{RB} = 2S_B^{\,3}\left[\frac{S_B\,(0.5\alpha - 0.828) + 0.828}{S_B\,(\alpha - 0.414) + 0.414}\right] \tag{18}$$

It might be felt that the assumptions underlying the derivation of equation (18) provide a poor description of the hydromechanics of an eddy swirl, but it can be shown that in some important cases this defect is of second-order importance (fig. 9). Also, the data of Ellis and Gay (1959) support use of equation (18).

Equation (18) yields:

$$K_{RB} = \frac{2S_B^{\,3}\,[S_B\,(0.5\alpha - 0.82) + 0.82]}{\left(\frac{Li}{3L}\right)[(S_B\{\alpha - 0.41\} + 0.41) + 4(S_B\{.5\alpha - .82\} + .82)] + \left(\frac{L-Li}{L}\right)[2S_B\,(.5\alpha - .82) + 1.64]} \tag{19}$$

when Li/L values less than unity are to be assumed, since the resistance to flow of phase B through that portion of the crack where the fluid-fluid interface exists is:

$$\frac{Li}{3t^3M} + \frac{2Li}{t^3N} = \frac{(\Delta P)_{Li}W}{12Q_B\mu_B} \tag{20}$$

and the resistance to flow of phase B through that portion of the crack where no fluid-fluid interface exists is:

$$\frac{(L - Li)}{t^3N} = \frac{W\,\Delta P_{(L - Li)}}{12Q_B\mu_B} \tag{21}$$

In equations (20) and (21), ΔP is the pressure drop across Li or (L - Li) as the case might be, M is the argument of equation (18), and $N = S_B^{\,3}$ (the argument of equation [12] when μ is zero). Thus, equation (19) is derived as equation (15) was derived from equation (14), in the manner first suggested by Scott and Rose (1953).

Using the functions of equation (16), and setting:

$$(Ai/A_T)_N = 1.67\,(1 - S_N)$$

and $$(A_s/A_T)_N = 1.67\,S_N - 0.67 \tag{22}$$

where the subscript, N, identifies the B fluid to be considered as the nonwetting phase.

Figure 9 can be derived from equation (19) to show the apparent second-order dependence of relative permeability curves on viscosity ratio.

Although the conditions which have been imposed (equations [16] and [22]) may be arbitrary, they are qualitatively reasonable. Thus, equation (16) says that, when the wetting phase is decreasing in saturation, $(Ai/A_T)_A$ increases from the proper limit of zero to some maximum value, and $(A_S/A_T)_A$ decreases from the proper limit of unity and approaches zero. In a like manner, equation (22) gives the proper limits and proper trend for the nonwetting phase surface area functions as the wetting phase saturation increases.

In these latter connections, both figures 6 and 8 show that the greatest departures from Darcy's Law occur at the higher values for saturation ($S > 0.7$), which are in fact the ones plotted in figure 9. It is an arbitrary consequence of the geometry of the crack model, of course, that the Ai/A_T ratio varies from zero to 0.5, and the A_S/A_T ratio varies from unity to 0.5, as the Li/L ratio varies from zero to unity. This prevents consideration of the functions of equations (16) and (22) over the entire saturation range (from zero to unity). Inspection shows, however, that if the model could be treated to handle the lower saturation ranges (below $S_W \cong 0.3$ and $S_N \cong 0.7$), the dependence of relative permeability on viscosity ratio would be even less noticeable than the limits depicted in figure 9.

CONCLUSIONS

In this paper, use has been made of the self-evident, but sometimes overlooked, consideration that one fluid passing over another contiguous immiscible fluid will always impart a motion to the second fluid. This gives, in general, a non-zero velocity boundary condition to be imposed at the fluid-fluid interface, which must be used in the solution of the appropriate differential equations of motion. When streamline flow is being considered, the equations of motion are derived from the Stokes-Navier Law of Force, the Continuity Equation, and the thermodynamic Equation of State, and their solution may be taken as properly describing the flow transfer process.

These methods have been applied herein to one-dimensional, two-phase flow of stratified liquids in a capillary space having the geometry of a wide crack with parallel surfaces. Figure 1 shows this model, with the oppositely located source and sink, and the parallel and impermeable edge boundaries in the direction of flow. For flow in the viscous regime, this model may be taken to represent a porous medium prototype such as the petroleum reservoir sedimentary rock system through which oil and water are flowing. By introducing the parameter, (Li/L), a better representation is obtained, as shown by figures 1 and 4, since the model can then be scaled to show a particular dependence of the amount of interfacial (fluid-fluid) surface area on the fluid saturation parameters, S_A and S_B.

Evidently the models of figures 1 and 4 can be taken to represent other prototypes of mixture flow systems as encountered in other branches of engineering (for example, pipeline transport of oil lubricated by the presence of an aqueous phase, two-phase flow in catalytic reactors, transport of condensate films by moving vapor, etc.).

This paper includes results for the cases where an equal driving force acts directly on each of the stratified fluids, where the driving force acts only on one fluid and the other is simply dragged along, and where the driving force acts only on one fluid and the other is caused to rotate in an eddy swirl.

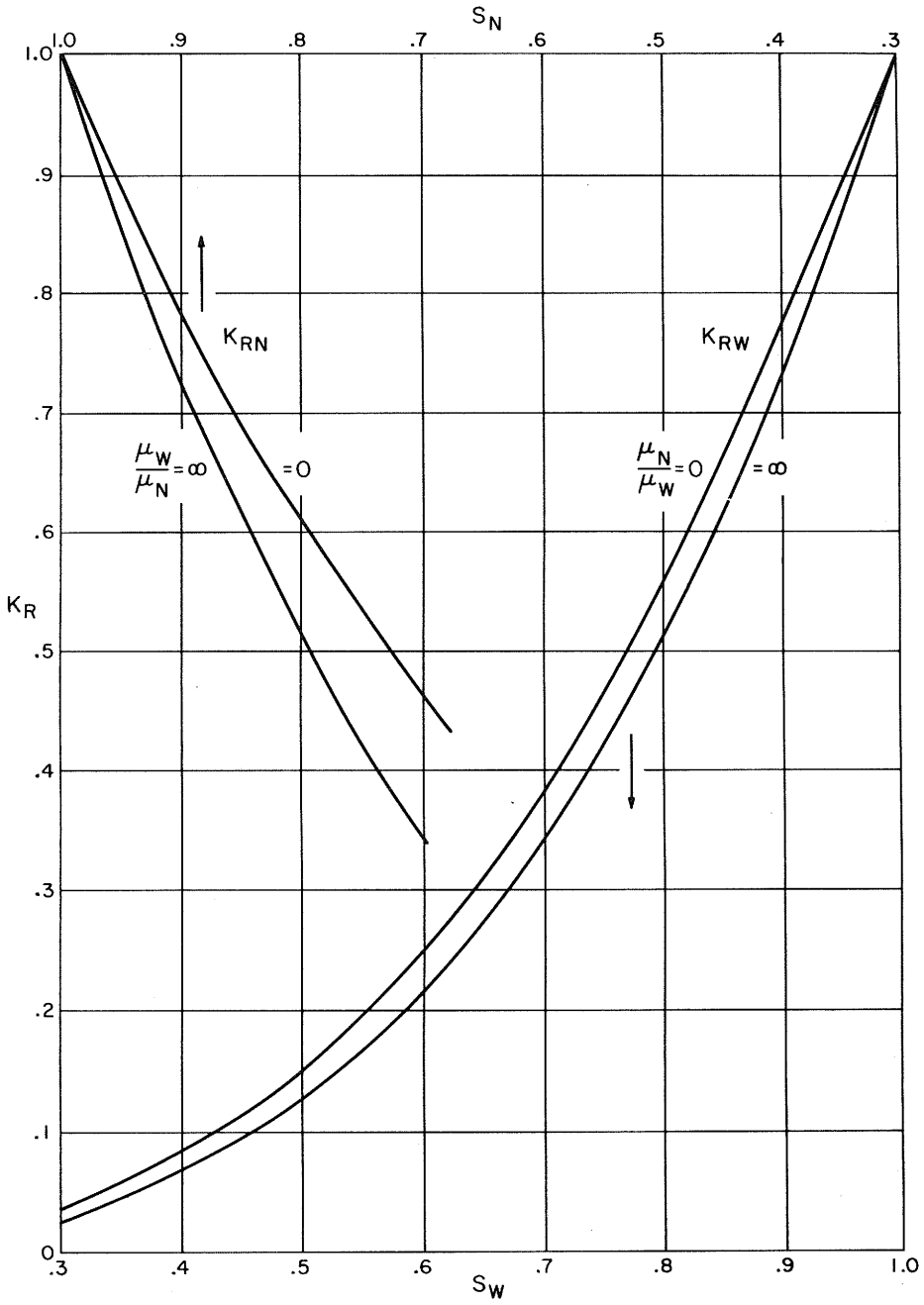

Fig. 9. Relative permeability curves for wetting and nonwetting phases for the model of figure 4 in a special case, showing the second-order dependence on viscosity ratio.

Other cases of importance, (not treated herein, but derivable by the analytic methods which are presented) are those in which unequal driving forces act on each of the stratified fluids, and those in which equal (or unequal) but oppositely directed driving forces act on each fluid.

Figures 2, 3, and 5 show the magnitude of the lubrication effect as a function of the viscosity ratio, and it is seen that the maximum velocity increase occurs for a particular fluid when the viscosity of the contiguous fluid is the least. It is also apparent from these curves that there is an energy loss (an increase in the power requirement) whenever the driving force acts on only one (instead of both) of the moving fluids, and that this effect is greatest when the rotational swirl is assumed to develop.

Figures 6 and 8 also express the magnitude of the lubrication effect, by relating the relative permeability parameter to saturation and to viscosity ratio parameters. From these it may be concluded that the volumetric throughput of a particular fluid that only partially fills the capillary pore space is sometimes greater than its throughput when it completely fills the pore space. This condition of increased conductivity is met when the saturation of the fluid approaches unity, as long as the contiguous fluid has a lower viscosity. For example, figure 6 indicates that the more viscous fluid need fill no more than 60 percent of the pore volume in order to have a conductivity greater than when it fills 100 percent of the pore volume, as long as the viscosity ratio (least viscous to the most viscous fluid) is of the order of 0.1, and as long as the fluid-fluid interface extends along the entire flow path.

Of special importance to the matter of oil recovery are the indications of the curves of figures 7 and 9. These suggest that the relative permeability versus saturation functions do have a dependence upon the viscosity ratio as long as finite fluid-fluid interfacial boundaries characterize the prototype reservoir rock system. Even though this dependence may prove to be a second-order effect in some cases, thus explaining why previously obtained experimental data have not shown the dependence, it must be concluded that Darcy Law interpretations have limited application to mixture flow phenomena. This is because an implicit assumption made in the statement of Darcy's Law is that flowing fluids have zero velocities at all fluid-fluid and fluid-solid boundaries, in unnecessary contradiction to the elementary premise of the analyses of this paper, which states that viscous forces extend across all fluid-fluid boundaries.

REFERENCES

Ellis, S. R. M., and Gay, B., 1959, The parallel flow of two fluid streams: interfacial shear and fluid-fluid interaction: Trans. Inst. Chem. Engs., v. 37, p. 206-213.

Hall, Warren A., 1956, An analytical derivation of Darcy's equation: Trans. Am. Geophysical Union, v. 37, p. 185-188.

Lamb, Horace, 1932, Hydrodynamics, 6th ed., Cambridge Univ. Press, England.

Milne-Thompson, L. M., 1955, Theoretical hydrodynamics, 3rd edition, Macmillan Company, New York.

Muskat, Morris, 1949, Physical principles of oil production: McGraw-Hill Book Company, Inc., New York.

Rose, Walter, 1957a, Fluid flow in petroleum reservoirs. I. The Kozeny paradox: Ill. Geol. Survey Circ. 236.

Rose, Walter, 1957b, Fluid flow in petroleum reservoirs. II. Predicted effects of sand consolidation: Ill. Geol. Survey Circ. 242.

Russell, T. W. F., and Charles, M. E., 1959, Effect of the less viscous liquid in the laminar flow of two immiscible liquids: Canadian Jour. Chem. Eng., v. 37, p. 18-24, Feb.

Russell, T. W. F., Hodgson, G. W., and Govier, G. W., 1959, Horizontal pipeline flow of mixtures of oil and water: Canadian Jour. Chem. Eng., v. 37, p. 9-17, Feb.

Scott, P. H., and Rose, Walter, 1953, An explanation of the Yuster effect: Jour. Petroleum Technology, v. 5, sec. 1, p. 19-20, Nov.

Yuster, S. T., 1951, Theoretical considerations of multiphase flow in idealized capillary systems: Proc. Third World Petroleum Congress, v. II, p. 437-445, The Hague.

Illinois State Geological Survey Circular 291
18 p., 9 figs., 1960

CIRCULAR 291

ILLINOIS STATE GEOLOGICAL SURVEY

URBANA